

# Electrical Impedance Cardiography Using Artificial Neural Networks

AJITKUMAR P. MULAVARA, WILLIAM D. TIMMONS, MEERA S. NAIR, VINEET GUPTA,  
AMARESH A. R. KUMAR, AND BRUCE C. TAYLOR

Department of Biomedical Engineering, The University of Akron, Akron, OH

(Received 12 August 1997; accepted 1 December 1997)

**Abstract**—This study evaluates the use of artificial neural networks to estimate stroke volume from pre-processed, thoracic impedance plethysmograph signals from 20 healthy subjects. Standard back-propagation was used to train the networks, with Doppler stroke volume estimates as the desired output. The trained networks were then compared to two classical biophysical approaches. The coefficient of determination ( $R^2 \times 100\%$ ) between the biophysical approaches and the Doppler was 8.20% and 9.90%, while it was 77.38% between the best neural network and the Doppler. Among these methods, only the neural network residuals had a significant zero mean Gaussian distribution ( $\alpha=0.05$ ). Our results indicate that an invertible relationship may exist between thoracic bioimpedance and stroke volume, and that artificial neural networks may offer a potentially advantageous approach for estimating stroke volume from thoracic electrical impedance, both because of their ease of use and their lack of confounding assumptions. © 1998 Biomedical Engineering Society. [S0090-6964(98)00304-X]

**Keywords**—Nonlinear processing, Noninvasive monitoring, Plethysmography, Cardiac output, Stroke volume.

## INTRODUCTION

Cardiac output (CO), defined as the volume of blood delivered by the heart per minute, is a major clinical measure of heart function and oxygen supply to the tissues. A decrease in cardiac output can cause low blood pressure, reduced tissue oxygenation, acidosis, poor renal function, and shock. In addition to clinical applications, decreased cardiac output can affect the health of otherwise normal individuals exposed to severe conditions and extreme environments. For example, jet pilots and astronauts routinely experience high and low gravities (G's). Astronauts especially are placed at risk by suddenly returning to Earth's 1 G environment after long exposures to microgravity. In these cases, decreased CO may cause black-outs, dizziness, nausea, and poor judgment — problems that may jeopardize a mission during

an emergency egress.<sup>3</sup> For these and other situations, an accurate, light weight, and easy-to-use CO monitor would have substantial benefits.

Thermodilution<sup>14</sup> and other indicator dilution methods<sup>8</sup> are available for accurate and reliable measurement of stroke volume (SV), but these techniques are invasive, require a trained physician and use expensive equipment. Doppler ultrasound<sup>5</sup> is widely used in hospital environments, it is noninvasive, and does not require a sterile environment. Like the dilution methods, unfortunately, it requires highly skilled technicians and expensive, bulky equipment.

Electrical impedance cardiography (EIC), another noninvasive technique, has strong correlations with the cardiac cycle (Figure 1). It promises to be accurate, inexpensive, compact, and user-friendly.<sup>1,10,16,18,20</sup> However, some investigators claim that EIC is nonrepeatable and inaccurate (e.g., see Refs. 4 and 6). One of the authors' own evaluations of a commercial EIC device and several published algorithms confirmed these negative findings.<sup>22</sup> Others suggest that EIC may be useful for routine screening.<sup>6</sup>

Given these contradictory findings we postulated that the relationship between thoracic impedance and SV may be too complicated for a simplified first-principles analysis as used in earlier investigations. In this paper, we explore the use of an artificial three-layer feed-forward neural network to define the relationship between thoracic electrical impedance and SV. Since an artificial network forms a nonlinear black box, it avoids the simplification errors associated with the earlier methods.

## BACKGROUND

In his seminal work, Nyboer<sup>19</sup> demonstrated that, for a uniformly shaped isotropically conducting volume  $\Delta V$ , a change in volume ( $\text{cm}^3$ ) is linearly related to  $\Delta Z$  — a change in electrical impedance ( $\Omega$ ) — by

$$\Delta V = - \left( \frac{\rho L^2}{Z_0^2} \right) \Delta Z, \quad (1)$$

Address correspondence to Bruce C. Taylor, Ph.D., Department of Biomedical Engineering, The University of Akron, Akron, OH, 44325-0302. Electronic mail: btaylor@brain.biomed.uakron.edu

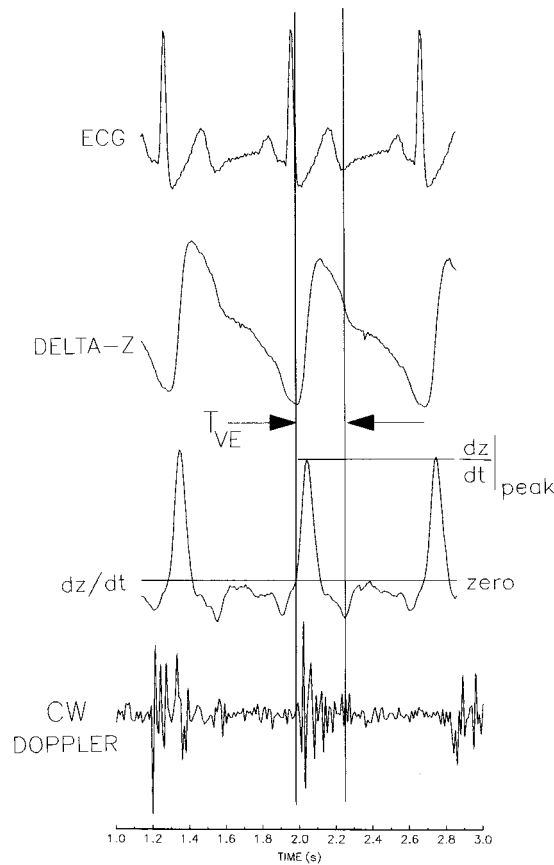


**FIGURE 1.** A sample of ECG, delta-Z, dz/dt, and CW Doppler tracings during the cardiac cycle showing the temporal relationships of these events. The figure demonstrates that the ejection phase of systole begins with the first zero-crossing of the dz/dt signal and terminates at the first negative peak following the R-spike of the ECG. The CW Doppler tracing is derived from the audio signal that results as a difference in frequency between the incident and reflected sound. This signal, recorded at the supra-sternal notch, shows when blood is ejected into the aortic arch and demonstrates a good correlation with the landmarks used to determine ventricular ejection time ( $\tau_{VE}$ ).

where  $\rho$  is the resistivity of the conductor ( $\Omega$  cm),  $L$  is the distance between the voltage sensing electrodes (cm), and  $Z_0$  is the mean basal impedance between these electrodes ( $\Omega$ ).

When Nyboer's methods were later applied to the human thorax, the impedance signal displayed a periodic pulsation that was strongly correlated with ventricular ejection (Figure 1).<sup>2,9,10-12</sup> These correlations have led several investigators to propose an inverse mapping, relating thoracic impedance to SV.

#### The Kubicek SV Estimator

Kubicek *et al.*<sup>10</sup> used the product of  $\tau_{VE}$  (s) (ventricular ejection time) and  $|dz/dt|_{\text{peak}}$  [the maximum value of the first derivative of impedance ( $\Omega/s$ )] to approximate

the impedance change due to blood ejection by the heart. Assuming the thorax was adequately modeled as a uniformly perfused cylinder, they estimated stroke volume by

$$K_{SV} = \frac{\rho L^2 \left| \frac{dz}{dt} \right|_{\text{peak}} \tau_{VE}}{Z_0^2}. \quad (2)$$

#### The Sramek SV Estimator

Sramek<sup>21</sup> and Bernstein<sup>2</sup> approximated the geometry of the thorax as a truncated cone rather than a cylinder cone, and both empirically related the subject's height and weight to  $V_{EPT}$ , the volume of electrically participating thoracic tissue ( $\text{cm}^3$ ). Hence, each replaced  $(\rho L^2/Z_0)$  with their own estimate of  $V_{EPT}$ , and obtained

$$S_{SV} = \frac{V_{EPT} \tau_{VE} \left| \frac{dz}{dt} \right|_{\text{peak}}}{Z_0}. \quad (3)$$

Sramek's estimate of  $V_{EPT}$  was based on anthropometry, for which the chest circumference was approximated as three times the distance between the voltage sensing electrodes. For this paper, we used Sramek's  $V_{EPT}$  as calculated by the Bomed NCCOM3 impedance cardiograph (see Experimental Methods below).

#### Neural Networks

Standard feed-forward networks consist of three layers of neurons (e.g., see Figure 2). Each neuron typically applies a transfer function, such as an hyperbolic tangent, to its weighted sum of inputs. Three-layer feed-forward networks can be used to identify nonlinear processes and models using gradient descent algorithms. The net in Figure 2 has a single neuron in the top layer (whose output is SV); four neurons in the input layer (each corresponding to an attribute of the thoracic impedance signal); and five neurons in the hidden layer. Hence, these nets can be conveniently interpreted as nonparametric, nonlinear, black box estimators.<sup>7</sup>

#### Importance of Bioimpedance Variables

The bioimpedance variables used to estimate the stroke volume as derived by classic biophysics analysis are related to important physiological parameters. The  $|dz/dt|_{\text{peak}}$  variable was shown to be related to the speed and force of ventricular contraction.<sup>12</sup> More recently, Kubicek<sup>9</sup> found that the peak value of the ventricular ejection velocity occurred concurrently with  $|dz/dt|_{\text{peak}}$ . This was the case even though the voltages sensed by the

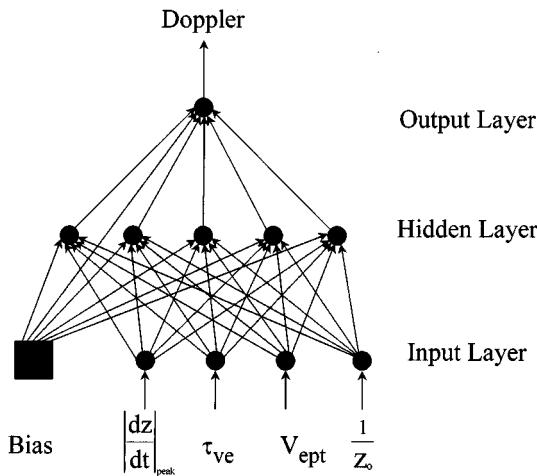


**FIGURE 2.** Example of a standard three-layer feed forward network. Inputs are weighted at the hidden layer and the hidden layer neurons are weighted at the output layer.  $|dz/dt|_{\text{peak}}$  is the maximum value of the first derivative of impedance ( $\Omega/s$ ),  $\tau_{VE}$  is the ventricular ejection time (s),  $V_{EPT}$  is the volume of electrically participating thoracic tissue ( $\text{cm}^3$ ),  $Z_0$  is the mean basal impedance between these electrodes ( $\Omega$ ) and Bias is a constant.

electrodes placed on the neck and the lower thorax measure a total impedance change that was a complex integration of the impedance changes from the aortic valve to the descending aorta. Bernstein<sup>2</sup> concluded that as long as (a) the total left ventricular output is not redistributed, (b) the mean basal impedance is constant, and (c) the distance between the sensing electrodes is fixed, the  $|dz/dt|_{\text{peak}}$  reflects changes in peak ascending aortic blood flow and velocity.

The mean basal impedance ( $Z_0$ ) has been related to the amount of fluid in the thorax.<sup>1,11,16</sup> Meijer *et al.*<sup>17</sup> found the derivative of  $Z_0$ , with respect to the interelectrode distance, to be a satisfactory estimate of thoracic fluid volume. Roos *et al.*<sup>20</sup> showed that a relationship existed between the mean basal impedance normalized by the interelectrode distance with the total extracellular fluid volume in normal volunteers and ambulatory patients. Further, Berman *et al.*<sup>1</sup> suggested that the sensitivity of the bioimpedance method was comparable to other methods used in monitoring intrathoracic fluid volume changes.

## EXPERIMENTAL METHODS

### Data Collection

Simultaneous impedance and Doppler echo velocimetry data were obtained from 20 healthy normal subjects. Details of the experimental methods, protocols, and data postprocessing may be found in Taylor.<sup>22</sup> The subject population consisted of ten healthy males and ten healthy females ranging in age from 24 to 50 years (mean

$30.7 \pm 6.9$  years). Subject heights ranged from 1.49 to 1.88 m (mean  $1.68 \pm 0.1$  m) with weights ranging from 50 to 95 kg (mean  $67.80 \pm 15.61$  kg).

Following standard procedures, thoracic bioimpedance was measured with the Bomed NCCOM3 impedance cardiograph (Bomed Medical Manufacturing, Ltd., Irvine, CA 92718) and stroke volume was measured with the Biosound Genesis II Echo Cardiograph (Biosound Corporation, Indianapolis, IN 46250). The respiratory artifacts were minimized by utilizing breath-holds during measurements. For each subject, six data sets were collected for three supine body positions (horizontal,  $10^\circ$  head down, and  $30^\circ$  head up) and recorded on a TEAC analog tape recorder (Teac, America Inc., Montebello, CA 90640) for later analysis. The 360 ( $20 \times 6 \times 3$ ) post-processed data sets included the following parameters: L,  $V_{EPT}$ ,  $Z_0$ ,  $|dz/dt|_{\text{peak}}$ ,  $\tau_{VE}$ , SV (Doppler), heart rate, patient height, weight, age, and gender.

### Kubicek and Sramek SV Calculation

Equations (2) and (3) were used to calculate the Kubicek ( $K_{SV}$ ) and Sramek ( $S_{SV}$ ) estimates of SV.

### Neural Network SV Calculation

Eight standard three-layer feed-forward neural networks were designed, trained, and tested using NeuralWare Professional II Plus (NeuralWare Inc., Pittsburgh, PA 15276). First, the input and the desired output data were transformed so that each variable had zero mean and near unity bipolar range ( $-1, +1$ ). The 360 data sets were then randomized and split into a training and testing group ( $n=180$  each). Three basic types of networks were implemented based on their inputs (see Table 1): the NNK (neural net, Kubicek) type used variables common to Equation (2) (Kubicek's estimator); the NNS (neural net, Sramek) type used variables common to Equation (3) (Sramek's estimator); and the EIC type used variables common to both. The desired output of each net was the Doppler-estimated SV.

For each network, a hyperbolic tangent transfer function was used for the input and hidden layer neurons, while the output layer used a linear transfer function. Standard back-propagation was used to train each network, with two stopping criteria: root mean squared (rms) error (0.001) and maximum iteration count (999,999). The number of hidden neurons in each network was optimized by trial and error. Once trained, the testing data were used to compare the outputs of the network models (transformed back to full scale and offset) with the corresponding Doppler SV.

### Goodness of Fit

A regression analysis was performed for each impedance SV method versus Doppler. The coefficient of de-

**TABLE 1. Neural network designs.**  $|dz/dt|_{\text{peak}}$  is the maximum value of the first derivative of impedance ( $\Omega/s$ ),  $\tau_{VE}$  is the product of the ventricular ejection time (s),  $V_{EPT}$  is the volume of electrically participating thoracic tissue ( $\text{cm}^3$ ),  $L$  is the distance between the voltage sensing electrodes (cm) and  $Z_0$  is the mean basal impedance between these electrodes ( $\Omega$ ).

Network	Input parameters	Termination criterion	Hidden PEs
EIC1	$\left  \frac{dz}{dt} \right _{\text{peak}}$ ; $\tau_{VE}; V_{EPT}; L^2; 1/Z_0$ ; $1/(Z_0)^2$	Maximum iteration count	11
EIC2	$\left  \frac{dz}{dt} \right _{\text{peak}}$ ; $\tau_{VE}; V_{EPT}; L^2; 1/Z_0$ ; $1/(Z_0)^2$	rms error	05
EIC3	$\left  \frac{dz}{dt} \right _{\text{peak}}$ ; $\tau_{VE}; L; Z_0$	Maximum iteration count	09
EIC4	$\left  \frac{dz}{dt} \right _{\text{peak}}$ ; $\tau_{VE}; L; Z_0$	rms error	07
NNK1	$\left  \frac{dz}{dt} \right _{\text{peak}}$ ; $\tau_{VE}; L^2; 1/(Z_0)^2$	rms error	07
NNK2	$\left  \frac{dz}{dt} \right _{\text{peak}}$ ; $\tau_{VE}; L^2; 1/(Z_0)^2$	Maximum iteration count	08
NNS1	$\left  \frac{dz}{dt} \right _{\text{peak}}$ ; $\tau_{VE}; V_{EPT}; 1/Z_0$	rms error	03
NNS2	$\left  \frac{dz}{dt} \right _{\text{peak}}$ ; $\tau_{VE}; V_{EPT}; 1/Z_0$	Maximum iteration count	05

termination  $[(CD)=R^2 \times 100\%]$ , the mean error (ME), the standard error of the mean (SEM), and the rms error were calculated. Akaike's final prediction error (FPE)<sup>15</sup> (which modifies the rms error to account for parsimony) was also determined along with the skewness of the residuals ( $n=180$  for the Kubicek and Sramek equations and the networks). The skewness was tested for significance with respect to its deviation from a normal distribution (skewness=0) at  $\alpha=0.05$ .

## RESULTS

The network structures, the stopping criterion, and the optimized number of hidden layer neurons are shown in Table 1. Regressions between the SV estimates from bioimpedance and Doppler methods are shown in Figure 3, and the resulting slopes, intercepts, CDs, and standard

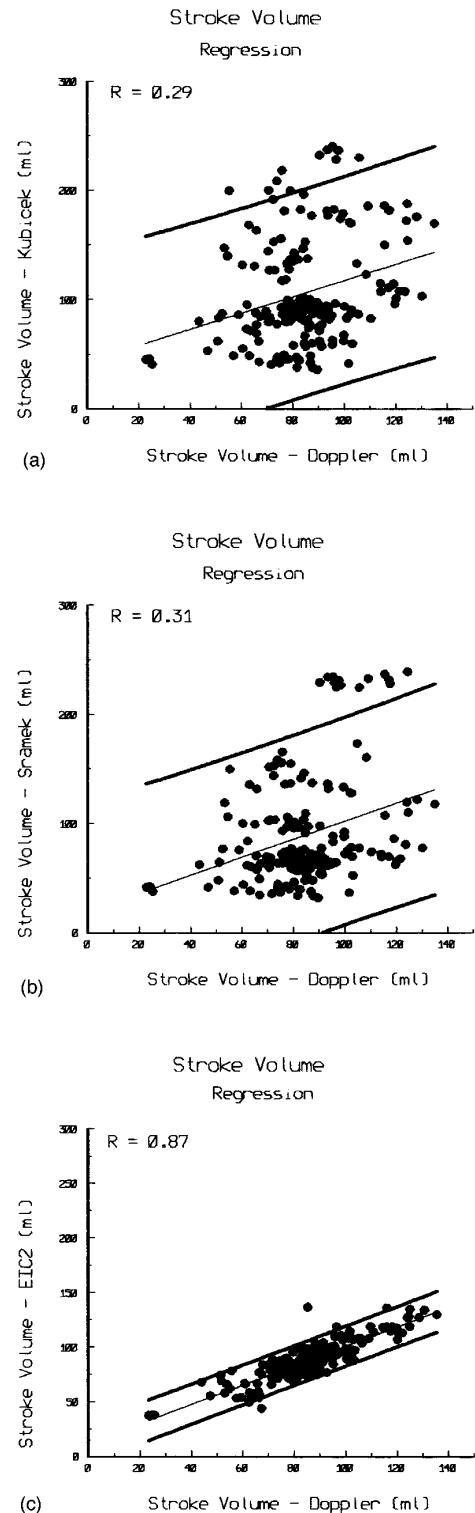


**FIGURE 3. Exemplar results of regression analysis.** The thick lines indicate the 95% confidence limits for the regression. The correlation coefficient is indicated. (a),(b) Results of the regression analysis of classical biophysics estimates (Kubicek and Sramek) of stroke volume with Doppler. (c) Results of the regression analysis of the best network estimate of stroke volume with Doppler.

**TABLE 2. Results of regression analysis between the Doppler stroke volume and predicted model estimates.**

Stroke volume measurement	Slope	Intercept (ml)	Coefficient of determination $R^2 \times 100\%$	Standard error of the estimate
Kubicek	0.74	42.94	08.20	47.96
Sramek	0.83	19.40	9.90	47.96
EIC1	0.94	03.01	76.54	10.01
EIC2	0.88	12.50	77.38	09.18
EIC3	0.79	18.23	68.64	10.32
EIC4	0.93	04.10	58.27	15.13
NNK1	0.83	12.20	56.94	13.82
NNK2	0.80	12.68	73.23	09.26
NNS1	0.54	40.00	47.06	10.98
NNS2	0.67	26.69	59.26	10.68

error of the estimates are listed in Table 2. Note that the EIC2's CD is nearly seven times larger than the CD of the Kubicek and Sramek estimators.

ME, SEM, rms, skewness, and FPE for each method are listed in Table 3, and histograms of the residuals are shown in Figure 4. Note that the rms error of the Kubicek and Sramek estimators were five times larger than the networks. Based on skewness, the residuals of the Kubicek and Sramek SV estimators [Figure 4(a)] showed a significant deviation from a normal distribution ( $\alpha = 0.05$ ), while all the networks except for the NNK1 [Figure 4(b)] showed no significant deviation ( $\alpha = 0.05$ ).

**DISCUSSION**

The cardiac contraction and the associated ejected blood and fluid redistribution affect thoracic bioimpedance (the forward problem). However, it remains to be seen whether the ejected blood volume can be determined reliably from thoracic bioimpedance (the inverse problem). The Kolomogorov and Universal Approximation theorems for neural networks allow one to avoid

**TABLE 3. Descriptive statistics for the residuals, where the residuals are the differences between the Doppler and the predicted values of stroke volume.**

Model	Mean (ml)	Standard error of mean (ml)	Standard deviation of mean (ml)	rms error (ml)	FPE
Kubicek	-21.24	3.58	48.07	52.435	1374.69
Sramek	-04.58	3.57	47.94	48.029	1153.38
EIC1	+01.96	0.75	10.04	10.211	131.85
EIC2	-02.61	0.70	09.41	09.748	075.53
EIC3	-00.79	0.82	11.01	11.012	113.98
EIC4	+01.77	1.13	15.15	15.209	173.49
NNK1	+02.47	1.06	14.17	14.348	154.41
NNK2	+04.53	0.75	10.01	10.967	105.12
NNS1	-00.85	1.05	14.07	14.055	118.04
NNS2	+01.29	0.92	12.38	12.413	109.09

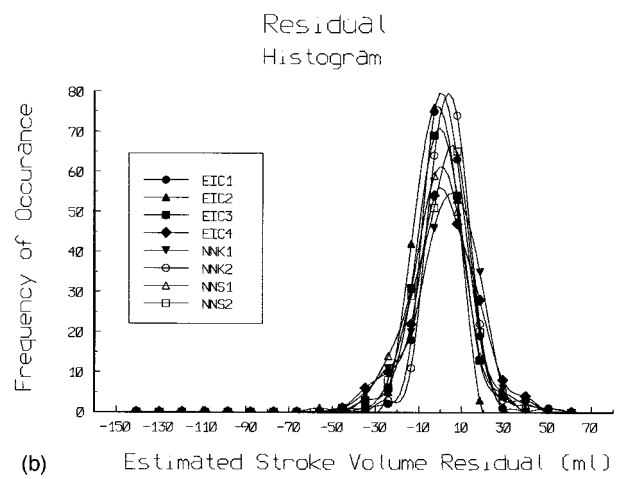
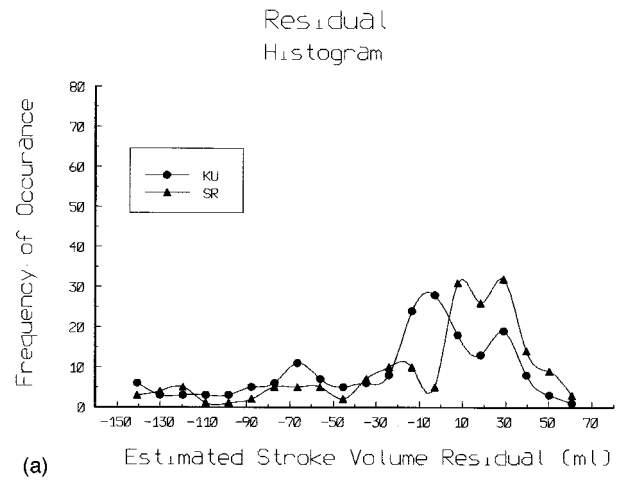


**FIGURE 4. Histograms of the residuals, where the residuals are defined as the Doppler stroke volume minus the predicted stroke volume. (a) Residuals from classical biophysics predictions. (b) Residuals from neural network predictions. For clarity, smooth curves are drawn through the midpoint values of each discrete bin. Bins are 10.6 ml each.**

some of the simplifications necessary for a classical biophysics approach; the results from this study lend credence to this nonlinear black box approach. The classic biophysics approaches (the Kubicek and Sramek estimators) performed poorly, explaining only 8%–10% of the variability in the Doppler SV estimate, while the neural network EIC2 explained 77%. Similarly, the rms error and FPE were likewise poor for the two biophysics-based estimators as compared to the EIC2 (Table 3). The rms for the worst neural net measured at least three times better than the Kubicek and Sramek estimators. The poor performance of the Kubicek and Sramek predictors is also reflected in the skewness of their residuals. All but one of the neural networks, on the other hand, produced normally distributed residuals ( $\alpha = 0.05$ ). Of these, EIC2

had the largest CD, the smallest rms error, and the smallest FPE. Even though the EIC2 had the largest number of inputs of all the nets, it required only a small number of hidden neurons.

We also observed that, as fewer assumptions and constraints were imposed on the neural models, their performance improved. For example, consider net EIC1: 11 hidden neurons were required to map the inverse function. EIC2, on the other hand, used the same inputs, but with  $|dz/dt|_{\text{peak}}$  and  $\tau_{\text{VE}}$  provided separately instead of pre-multiplied: it only required five hidden neurons and produced an even better rms error. If this observation is correct, it may be beneficial to also break  $V_{\text{EPT}}$  into its constituent parts: gender (which has a well known effect on SV), chest circumference, height, weight, and build (length between electrodes is already provided). Inclusion of body position (tilt) may also have improved the performance since the data were specifically collected to elucidate tilt effects. However, if tilt were included, it would complicate any practical EIC design, since it would require extra sensors on the body. Hydration is another factor that may help the net, but it also would require extra sensors and complicate the design (tilt and hydration were factors not considered in this analysis). It may be possible to completely remove constraints and assumptions from the SV calculations by using the raw impedance wave form itself as the input to a neural net. This would require a major restructuring of the network and is the topic of future work.

A major limitation of our study was its small size and narrow population. Also, the use of Doppler Echo Cardiography as the gold standard may be problematic because of its inherent variability. Future studies need to target a larger population of both healthy and diseased subjects and utilize a higher fidelity CO monitor (such as a Thermo-dilution cardiograph) instead of a Doppler Echo Cardiograph.

A neural network model that could accurately determine stroke volume based on impedance measurements would present a significant breakthrough in cardiology. An easy to use, inexpensive, portable cardiograph would have wide applications in the clinical setting, sports physiology, and space studies, to name a few, and potentially lead to improved patient care. However, further research is needed to clarify the reliability and scope of the neural solution.

## CONCLUSIONS

Our results indicate that an invertible relationship exists between thoracic bioimpedance and stroke volume. Furthermore, we have shown that artificial neural networks offer a potentially advantageous method for estimating SV from thoracic electrical impedance, both because of their ease of use and their lack of confounding

assumptions. The neural network approach showed a large improvement over classical biophysical approaches. The CD increased from a high of 10% for the first principle's approach to 77% for the best neural network. Still this neural approach needs to be cross validated with other high fidelity CO monitoring methods over a larger number of subjects as well as over a wider range of physiological variations such as tilt and hydration and nonstandard impedance wave forms.

## ACKNOWLEDGMENTS

The data collection was supported by the NASA/ASEE Summer faculty fellowship program 1993, Johnson Space Center, Houston, Texas, Contract No. NGT-44-001-800 to Bruce C. Taylor, Ph.D. (PI). The authors would like to acknowledge Janice Yelle, Todd Schlegel, Bill Fortner, Larry Dussack, Margie Wood, Donna South, Kristen Nichols, and Christopher Miller for their help during the data collection. Preliminary results were presented in Ref. 13.

## REFERENCES

- <sup>1</sup>Berman, I., W. Scheetz, E. Jenkins, and H. Hufnagel. Transthoracic electrical impedance a guide to intravascular overload. *Arch. Surg.* 102:61–64, 1971.
- <sup>2</sup>Bernstein, D. P. A new stroke volume equation for thoracic electrical bioimpedance: Theory and rationale. *Crit. Care Medicine* 14:904–909, 1986.
- <sup>3</sup>Churchill, S. E. Fundamentals of Space Sciences, Vol. 1. Malabar, FL: Kreiger, 1997.
- <sup>4</sup>Donovan, K., G. Dobb, W. Woods, and B. Hockings. Comparison of transthoracic electrical impedance and thermodilution methods for measuring cardiac output. *Crit. Care Medicine* 14:1038–1044, 1986.
- <sup>5</sup>Geddes, L. A. The Direct and Indirect Measurement of Blood Pressure. Chicago, IL: Yearbook Medical, 1970.
- <sup>6</sup>Handelsman, H. Cardiac output by electrical bioimpedance. *Health Technology Assessment Report* 3:1–5, 1989.
- <sup>7</sup>Haykin, S. Neural Networks — A Comprehensive Foundation. New York, NY: Macmillan College, 1994.
- <sup>8</sup>Judy, W., F. Langley, K. McCowen, D. Stinnett, L. Baker, and P. Johnson. Comparative evaluation of the thoracic impedance and isotope dilution methods for measuring cardiac output. *Aerospace Medicine* 40:532–536, 1969.
- <sup>9</sup>Kubicek, W. On the source of peak first time derivative ( $dz/dt$ ) during impedance cardiography. *Ann. Biomed. Eng.* 17:459–462, 1989.
- <sup>10</sup>Kubicek, W., A. From, R. Patterson, D. Witsoe, A. Castaneda, R. Lillehei, and R. Ersek. Impedance cardiography as a noninvasive means to monitor cardiac function. *J. Assoc. Adv. Medical Instrumen.* 4:79–84, 1970.
- <sup>11</sup>Kubicek, W., J. Karnegis, R. Patterson, D. Witsoe, and R. Mattson. Development and evaluation of an impedance cardiac output system. *Aerospace Medicine* 37:1208–1212, 1966.
- <sup>12</sup>Kubicek, W., J. Kottke, M. Ramos, R. Patterson, D. Witsoe, J. Labree, W. Remole, T. Layman, H. Schoening, and J. Garamela. The Minnesota impedance cardiograph— theory and applications. *Biomed. Eng.* 9:410–419, 1974.

- <sup>13</sup>Kumar, A. A. R., B. C. Taylor, A. P. Mulavara, M. S. Nair, V. B. Gupta, and W. D. Timmons. A Neural network approach to electrical impedance cardiography, In: Proceedings of the 16th Annual International Conference of the IEEE EMBS, Baltimore, Maryland, 1994.
- <sup>14</sup>Levett, J., and R. Replegle. Thermodilution cardiac output: a critical analysis and review of the literature. *J. Surg. Res.* 27:392–404, 1979.
- <sup>15</sup>Ljung, L. System Identification : Theory for the User. Englewood Cliffs, NJ: Prentice–Hall, 1987.
- <sup>16</sup>Luepker, R., J. Michael, and J. Warbasse. Transthoracic electrical impedance; quantitative evaluation of a non-invasive measure of thoracic fluid volume. *Am. Heart J.* 85:83–93, 1973.
- <sup>17</sup>Meijer, J., J. Reulen, P. Oe, W. Allon, L. Thijs, and H. Schneider. Differential impedance plethysmography for measuring thoracic impedance's. *Med. Biol. Eng. Comp.* 20:187–194, 1982.
- <sup>18</sup>Miller J., and S. Horvath. Impedance cardiography. *Psychophysiology* 15:80–91, 1978.
- <sup>19</sup>Nyober, J. Electrical Impedance Plethysmography. Springfield, IL: Thomas C.C., 1969.
- <sup>20</sup>Roos, J., H. Koomans, P. Boer, and E. D. Mees. Transthoracic electrical impedance as an index of extracellular fluid volume in man. *Intensive Care Medicine* 11:39–42, 1985.
- <sup>21</sup>Sramek, B. Cardiac output by electrical impedance. *Med. Electron.* 1982:93–97 (April).
- <sup>22</sup>Taylor, B. C. Evaluation of bioimpedance for the measurement of physiologic variables as related to hemodynamic studies in spaceflight. NASA Johnson Space Center, Houston, NASA/ASEE Summer Faculty Fellowship Program, 1993.